



# Hypoxia Induces Epithelial-Mesenchymal Transition in Follicular Thyroid Cancer: Involvement of Regulation of Twist by Hypoxia Inducible Factor-1 $\alpha$

Yeon Ju Yang<sup>1,2</sup>, Hwi Jung Na<sup>1</sup>, Michelle J. Suh<sup>1</sup>, Myung Jin Ban<sup>1</sup>, Hyung Kwon Byeon<sup>1</sup>, Won Shik Kim<sup>1</sup>, Jae Wook Kim<sup>3</sup>, Eun Chang Choi<sup>1</sup>, Hyeong Ju Kwon<sup>4</sup>, Jae Won Chang<sup>1</sup>, and Yoon Woo Koh<sup>1</sup>

Departments of <sup>1</sup>Otorhinolaryngology and <sup>4</sup>Pathology, Yonsei University College of Medicine, Seoul;

<sup>2</sup>Brain Korea 21 PLUS Project for Medical Science, Yonsei University College of Medicine, Seoul;

<sup>3</sup>Department of Otorhinolaryngology-Head and Neck Surgery, Soonchunhyang University College of Medicine, Seoul, Korea.

**Purpose:** Although follicular thyroid cancer (FTC) has a relatively fair prognosis, distant metastasis sometimes results in poor prognosis and survival. There is little understanding of the mechanisms contributing to the aggressiveness potential of thyroid cancer. We showed that hypoxia inducible factor-1 $\alpha$  (HIF-1 $\alpha$ ) induced aggressiveness in FTC cells and identified the underlying mechanism of the HIF-1 $\alpha$ -induced invasive characteristics.

**Materials and Methods:** Cells were cultured under controlled hypoxic environments (1% O<sub>2</sub>) or normoxic conditions. The effect of hypoxia on HIF-1 $\alpha$ , and epithelial-to-mesenchymal transition (EMT) related markers were evaluated by quantitative real-time PCR, Western blot analysis and immunocytochemistry. Invasion and wound healing assay were conducted to identify functional character of EMT. The involvement of HIF-1 $\alpha$  and Twist in EMT were studied using gene overexpression or silencing. After orthotopic nude mouse model was established using the cells transfected with lentiviral shHIF-1 $\alpha$ , tissue analysis was done.

**Results:** Hypoxia induces HIF-1 $\alpha$  expression and EMT, including typical morphologic changes, cadherin shift, and increased vimentin expression. We showed that overexpression of HIF-1 $\alpha$  via transfection resulted in the aforementioned changes without hypoxia, and repression of HIF-1 $\alpha$  with RNA interference suppressed hypoxia-induced HIF-1 $\alpha$  and EMT. Furthermore, we also observed that Twist expression was regulated by HIF-1 $\alpha$ . These were confirmed in the orthotopic FTC model.

**Conclusion:** Hypoxia induced HIF-1 $\alpha$ , which in turn induced EMT, resulting in the increased capacity for invasion and migration of cells via regulation of the Twist signal pathway in FTC cells. These findings provide insight into a possible therapeutic strategy to prevent invasive and metastatic FTC.

**Key Words:** Hypoxia, hypoxia inducible factor-1 $\alpha$ , epithelial-mesenchymal transition, Twist, orthotopic thyroid cancer model, follicular thyroid cancer

**Received:** December 4, 2014 **Revised:** February 9, 2015

**Accepted:** February 11, 2015

**Co-corresponding authors:** Dr. Jae Won Chang, Department of Otorhinolaryngology, Yonsei University College of Medicine, 50-1 Yonsei-ro, Seodaemun-gu, Seoul 03722, Korea.

Tel: 82-2-2228-3607, Fax: 82-2-393-0580, E-mail: strive1005@yuhs.ac and

Dr. Yoon Woo Koh, Department of Otorhinolaryngology, Yonsei University College of Medicine, 50-1 Yonsei-ro, Seodaemun-gu, Seoul 03722, Korea.

Tel: 82-2-2228-3607, Fax: 82-2-393-0580, E-mail: ywkohent@yuhs.ac

•The authors have no financial conflicts of interest.

© Copyright: Yonsei University College of Medicine 2015

This is an Open Access article distributed under the terms of the Creative Commons Attribution Non-Commercial License (<http://creativecommons.org/licenses/by-nc/3.0>) which permits unrestricted non-commercial use, distribution, and reproduction in any medium, provided the original work is properly cited.

## INTRODUCTION

Thyroid carcinoma is the fifth leading cancer worldwide, and its incidence is increasing,<sup>1</sup> and 95% of these cancers are follicular cell origin-papillary (PTC), follicular (FTC), or anaplastic thyroid cancers (ATC).<sup>2</sup> In spite of the optimistic survival rates for PTC and FTC, a subset of this population demonstrates resistance to therapy, including radioiodine, and a propensity for more aggressive tumors with higher rates of extracapsular spread to the strap muscle and recurrent laryngeal nerve, tracheal invasion, and metastasis to lymph nodes, as well as recurrence or distant metastasis.<sup>3,4</sup> In particular, FTC is more likely to produce distant metastases, leading to a poorer prognosis for

FTC patients compared with PTC patients.<sup>1</sup> Thus, it is necessary to identify the underlying mechanisms leading to increased aggressiveness of FTC and develop novel methods to prevent the aggressive features of invasion and metastasis in FTC.

Cancer invasion to surrounding tissues or metastasis to other organs requires multi-phase processes, including epithelial-to-mesenchymal transition (EMT),<sup>5</sup> and it is the principal cause of mortality in patients with malignancies.<sup>6</sup> Although EMT is a vital process for morphogenesis during embryonic development, it has been implicated in the invasiveness of malignancies.<sup>7</sup> During EMT, epithelial cells dedifferentiate, lose cell polarity and epithelial surface markers, express mesenchymal markers, display phenotypic alterations, and subsequently migrate and invade.<sup>8</sup> The molecular hallmarks for EMT are the downregulation of epithelial cell adhesion molecules, such as E-cadherin, and the upregulation of mesenchymal components, such as vimentin and N-cadherin.<sup>9</sup>

Accumulating evidence has demonstrated hypoxia to be an important trigger of tumor cell invasion or metastases via hypoxic activation cascades, including hypoxia-inducible factor (HIF)-1.<sup>10</sup> This molecule consists of an oxygen-sensitive alpha subunit (HIF-1 $\alpha$ ) and a constitutively expressed beta subunit (HIF-1 $\beta$ ). HIF-1 activates many downstream signals involved in angiogenesis (VEGF),<sup>11</sup> anaerobic metabolism (GLUT-1),<sup>12</sup> control of intracellular pH (CA-9),<sup>13</sup> DNA damage responses,<sup>14</sup> and proliferation (p21 and p27),<sup>15</sup> which are essential to cancer cell adaptation, survival, and progression to overcome the stressful conditions of hypoxia.<sup>16,17</sup> Hypoxia and HIF-1 $\alpha$  are associated with tumor aggressiveness and poor prognosis in many different types of cancers, including uterine, prostate, stomach, pancreas, breast, non-small cell lung, and nasopharyngeal cancers.<sup>18-20</sup> Moreover, the potential clinical importance of HIF-1 $\alpha$  as a novel therapeutic target in thyroid cancer was most recently suggested by various studies demonstrating its pathophysiological role in thyroid cancer progression, aggressiveness, and metastasis.<sup>16,21</sup> However, the underlying molecular mechanism of increased aggressiveness and the poor prognosis of thyroid cancers with HIF-1 $\alpha$  overexpression are not fully understood.

The purpose of this study was to identify HIF-1 $\alpha$  expression triggered by hypoxia and to explore whether HIF-1 $\alpha$  activation is important for inducing the EMT phenotype associated with tumor migration and invasion. To the best of our knowledge, this is the first study evaluating the relationship between HIF-1 $\alpha$  and EMT in thyroid cancer.

## MATERIALS AND METHODS

### Cell lines and reagents

Human follicular (FTC133 and MLI) and papillary (TPC1 and BCPAP) thyroid cancer cells were purchased from the American Type Culture Collection (Manassas, VA, USA), and human anaplastic thyroid cancer cells (FRO and 8505C) were kindly

provided by Dr. Kim (Ajou University, Suwon, Korea). The FTC133, MLI, and TPC1 cell lines were maintained in high-glucose Dulbecco's modified Eagle's medium (PAA, Pasching, Austria), while BCPAP, FRO, and 8505C cell lines were cultured in RPMI (Lonza, Wakersville, MD, USA) supplemented with 10% fetal bovine serum and penicillin-streptomycin at 100 U/mL (GIBCO, Carlsbad, CA, USA). The cells were cultured at 37°C with 5% CO<sub>2</sub> under humidified conditions.

### Exposure to hypoxia

To induce hypoxia, cells were placed in a sealed hypoxic incubator (Thermo Fisher Scientific, Rochester, NY, USA) and continuously gassed with a manufactured mixture of 1% O<sub>2</sub> with 5% CO<sub>2</sub>:N<sub>2</sub> balance (37°C) for the indicated times. Control cells were incubated under normoxic conditions (21% O<sub>2</sub>, 5% CO<sub>2</sub>, 37°C) for equivalent periods.

### Western blot analysis

Cells were lysed on ice in lysis buffer [10 mM Tris-HCl (pH 7.4), 100 mM NaCl, 1 mM EDTA, 1 mM EGTA, 1 mM NaF, 20 mM Na<sub>4</sub>P<sub>2</sub>O<sub>7</sub>, 2 mM Na<sub>3</sub>VO<sub>4</sub>, 1% Triton X-100, 10% glycerol, 0.1% SDS, 0.5% deoxycholate] (Invitrogen, Camarillo, CA, USA) supplemented with 1 mM phenylmethylsulfonyl fluoride and protease inhibitor cocktail (Sigma, St. Louis, MO, USA). Whole cell extracts (20  $\mu$ g/lane) were electrophoresed using 10% SDS-polyacrylamide gels and electrotransferred to polyvinylidene fluoride membranes (Millipore, Schwalbach, Germany) as described previously.<sup>3</sup> The following antibodies were used for Western blotting: anti-HIF-1 $\alpha$  (1:1000), -E-cadherin (1:500), -N-cadherin (1:500), -vimentin (1:1000), -Twist (1:1000), -Slug (1:1000), and GAPDH (1:1000). All antibodies were purchased from Cell Signaling Technology, Inc. (Danvers, MA, USA).

### Quantitative real-time PCR

Total RNA from cultured cells was extracted using TRIzol (Invitrogen, Burlington, ON, Canada) according to the manufacturer's instructions. Complementary DNA was prepared using random primers and MuL<sub>v</sub> reverse transcriptase (Roche, Basle, Switzerland) according to the manufacturer's instructions. Real-time PCR reactions were performed in triplicate using a 1:10 dilution of cDNA and the KAPA SYBR Fast ABI Prism 2X qPCR Master Mix on an ABI 7300 Real-Time PCR machine (Applied Biosystems, MA, USA). Data were collected and analyzed using the 7300 Real-Time PCR software. The relative quantification of the expressed genes was carried out using the comparative quantification method. All mRNA quantification data were normalized to GAPDH. The following primers were used: HIF-1 $\alpha$ : forward 5'-CTC AAA GTC GGA CAG CCT CA-3', reverse 5'-CCC TGC AGT AGG TTT CTG CT-3'; E-cadherin: forward 5'-TGC CCA GAA AAT GAA AAA GG-3', reverse 5'-GTG TAT GTG GCA ATG CGT TC-3'; vimentin: forward 5'-GAG AAC TTT GCC GTT GAA GC-3', reverse 5'-GCT TCC TGT AGG TGG CAA TC-3'; Twist: forward 5'-GGC GCT TTC TTT TTG GAC CT-3', re-

verse 5'-AGG AGA GAG CAG GAG GAC GG-3'

### Immunocytochemistry

Cells were cultured on microscope coverslips under hypoxic or normoxic conditions. After 16 h, slides were washed with phosphate-buffered saline (PBS), fixed for 20 min in 4% formaldehyde, and re-hydrated in PBS. After blocking for 45 min in 5% bovine serum albumin in PBS, the slides were incubated overnight at 4°C with polyclonal rabbit anti-HIF-1 $\alpha$ , -E-cadherin, and -vimentin antibodies (1:100; Cell Signaling Technology), washed with PBS, and incubated for 45 min with Alexa 488-labeled goat anti-rabbit antibodies or Alexa 568-labeled donkey anti-mouse antibodies (1:250; Molecular Probes, Inc., Eugene, OR, USA). The slides were washed with PBS and mounted using Duolink mounting medium with DAPI (Olink Bioscience, Sweden) and then analyzed using a LSM700 confocal microscope (Carl Zeiss Vision, Germany).

### Wound healing assay

To investigate cell migration, cells were plated in 6-well culture plates at a density of  $1 \times 10^5$ /well and grown to a subconfluent cell layer. When cells reached 90% confluence, a scratch was created in the cell monolayer using a sterile plastic pipette tip, and cells were washed twice with serum-free medium to remove cell debris. Mitomycin C (1  $\mu$ g/mL) was applied to cells to block the cell proliferation effect. After 16–24 h of incubation, migrated cells in the wounded area were visualized and photographed under an inverted microscope.

### Invasion (transwell) assay

Cell invasion under normoxic or hypoxic conditions was evaluated in Transwell chambers (24-well; Costar, Cambridge, MA, USA) as described previously.<sup>22</sup> Initially, fibronectin (2  $\mu$ g/filter) was dissolved in 100  $\mu$ L of minimal essential medium and poured into the upper section of the polyethylene filter (pore size, 8  $\mu$ m). The wells were coated overnight in a laminar flow hood, after which  $5 \times 10^5$  cells (in 100  $\mu$ L growth medium) were added to the top of the filter in the upper well. The chamber was incubated for 12 h under normoxic or hypoxic conditions with 5% CO<sub>2</sub> at 37°C. Non-migrant cells located in the upper section of the filter were removed using a cotton swab. Finally, attached cells in the lower section were stained with crystal violet and counted using a light microscope.

### HIF-1 $\alpha$ transfection

HIF-1 $\alpha$  overexpression was achieved by transfection with pcDNA3 HIF-1 $\alpha$ -HA (Addgene, Cambridge, MA, USA) using Fugene<sup>®</sup> HD Transfection (Promega, Madison, WI, USA) according to the manufacturer's recommended protocol. After transient transfection for 24 h, cells were cultured for 4 weeks. HIF-1 $\alpha$  positive cell clones were selected and expanded.

### Silencing of HIF-1 $\alpha$ (RNA interference)

Lentivirus-mediated short hairpin RNA (shRNA) silencing of

HIF-1 $\alpha$ : Stable FTC133 cells were generated by polybrene (Santa Cruz Biotechnology, Inc., CA, USA) transduction using HIF-1 $\alpha$  shRNA lentiviral particles (Santa Cruz Biotechnology, Inc., CA, USA). Cells expressing shRNA was obtained via selection with puromycin (5–10  $\mu$ g/mL). New media containing fresh puromycin were replaced every 3–4 days until the generation of resistant colonies.

### Orthotopic xenograft mouse model

Lentiviral control (LVcontrol) and shHIF-1 $\alpha$  FTC133 cells were harvested by trypsinization and washed with serum-free medium. After randomization into two groups (n=5), FTC133 cells ( $1 \times 10^5$ /5  $\mu$ L) were injected into the right thyroid lobe of 6-week-old male nude mice (Orientbio Inc., Seongnam, Korea) using a Hamilton syringe (Hamilton Company, Reno, NV, USA) and a 30-G needle as described previously.<sup>23</sup> The tumors were allowed to develop for 14 days. Animals were euthanized 28 days after implantation, and tumors were harvested. All of the animal experimental procedures were approved by the committee of ethics on animal research of the Yonsei University College of Medicine. All mice were treated in accordance to the guidelines for the care and use of laboratory animals of the institutional animal care and use committee of the institute.

Western blotting of HIF-1 $\alpha$ , E-cadherin, vimentin, and Twist was performed using samples from the specimens. The other half of the samples were fixed overnight in neutral buffered formalin, after which immunohistochemical staining of tumor tissues was performed using primary antibodies against E-cadherin, vimentin, and Twist as described previously.<sup>23</sup> The immunostained sections were analyzed under a Nikon light microscope. Microscopy images were captured using AxioCam digital microscope cameras and AxioVision image processing software (Carl Zeiss Vision, Germany).

### Statistical analysis

All data are represented as means $\pm$ SD from triplicate experiments. Student's t-tests and one-way ANOVAs were performed using SPSS 20.0 statistical software (SPSS, Chicago, IL, USA).  $p < 0.05$  was considered statistically significant (\* $p < 0.05$ ; \*\* $p < 0.01$ ; \*\*\* $p < 0.001$ ).

## RESULTS

### Hypoxia induces HIF-1 $\alpha$ expression in thyroid cancer cells

We examined the level of HIF-1 $\alpha$  expression in selected follicular (FTC133 and ML1), papillary (BCPAP and TPC1), and anaplastic thyroid cancer cells (8505C and FRO) under hypoxic conditions *in vitro*. As shown in Fig. 1A, all cell lines expressed relatively high levels of HIF-1 $\alpha$  protein after exposure to hypoxia. This was most prominent in FTC133 cells, which have lost PTEN expression. Consistent with hypoxia-induced HIF-1 $\alpha$

protein levels, HIF-1 $\alpha$  mRNA levels also increased under hypoxic conditions (Fig. 1B). Next, we determined the localization of HIF-1 $\alpha$  expression in each type of thyroid cancer using immunocytochemistry. Consistent with the immunoblotting and

RT-PCR results, the fluorescence of HIF-1 $\alpha$  was most strongly enhanced in FTC133 cells under hypoxic conditions and correlated with DAPI staining of the nucleus (Fig. 1C).

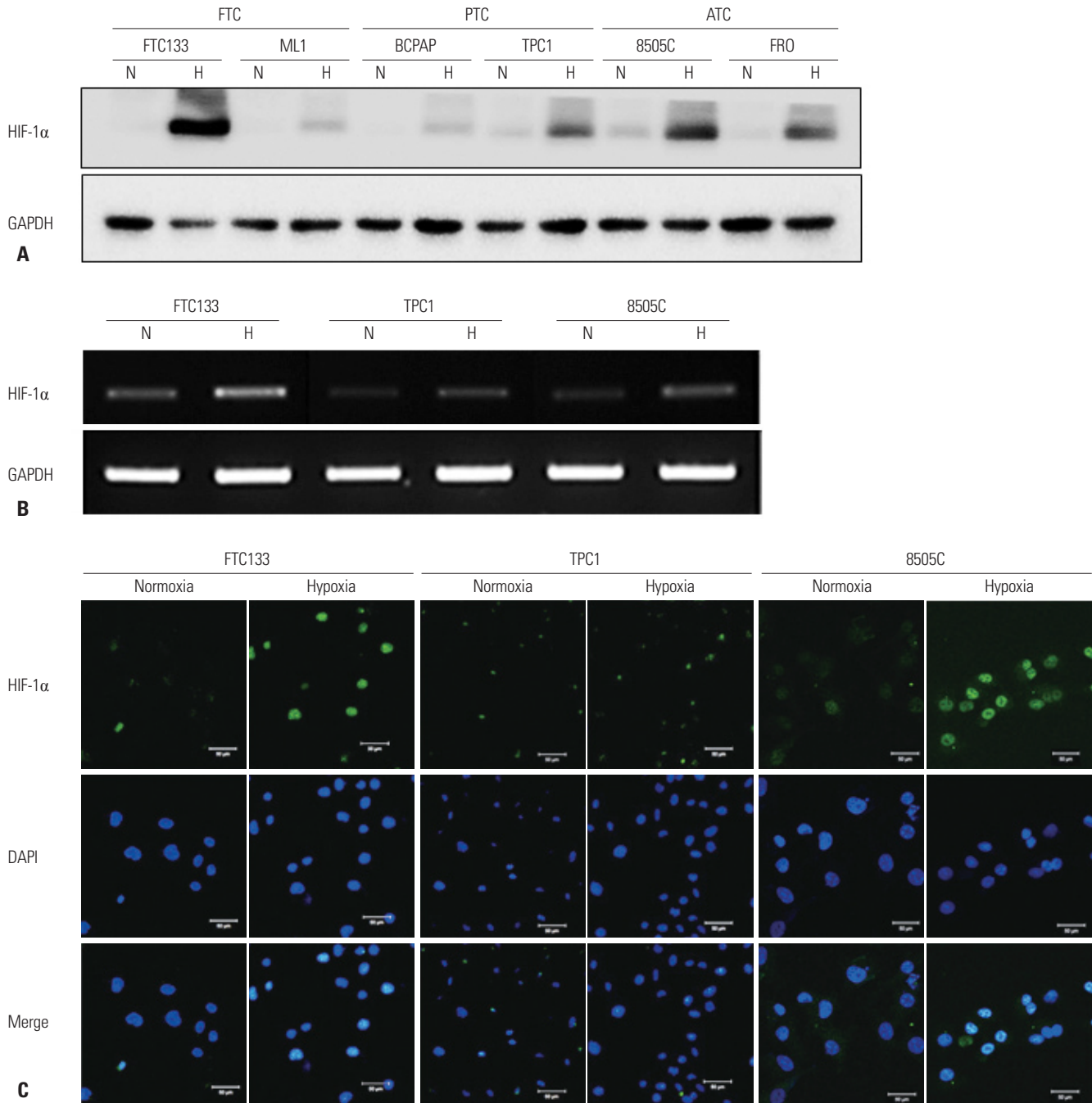


**Fig. 1.** Hypoxia-induced HIF-1 $\alpha$  expression in cell lines derived from different types of thyroid cancers. All cells were harvested after 16 h under normoxic or hypoxic conditions (1% O<sub>2</sub>), and HIF-1 $\alpha$  expression was analyzed using the following methods. (A) Western blot analysis of HIF-1 $\alpha$  in thyroid cancer cell lines derived from follicular (FTC133 and ML1), papillary (BCPAP and TPC1), and anaplastic (8505C and FRO) carcinomas. (B) Total RNA isolated from each selected thyroid cancer cell line. Cell lines with high protein expression of HIF-1 $\alpha$  under hypoxic conditions (FTC133, TPC1, 8505C) were analyzed for the presence of HIF-1 $\alpha$  transcripts using real-time PCR with primers specific for HIF-1 $\alpha$ . (C) Immunofluorescence staining of HIF-1 $\alpha$  expression in thyroid cancer cells. Cells were incubated under normoxic or hypoxic conditions for 16 hours, followed by immunofluorescence analysis. HIF-1 $\alpha$ , green; DAPI, blue. Hypoxia-induced HIF-1 $\alpha$  expression was highest in FTC133 cells. Scale bar=50  $\mu$ m. Each figure is representative of triplicate experiments. FTC, follicular thyroid cancer; PTC, papillary thyroid cancer; ATC, anaplastic thyroid cancer; HIF-1 $\alpha$ , hypoxia inducible factor-1 $\alpha$ .

## Hypoxia regulates epithelial-to-mesenchymal transition in thyroid cancer cells

To investigate whether hypoxia induces EMT in thyroid cancer cells, we first investigated the morphologic appearance of cancer cells under microscopy. All thyroid cancer cells (FTC133, TPC1, and 8505C) showed typical morphologic changes after

exposure to hypoxic conditions for 16 h, appearing flattened, spindle-shaped, and fibroblast-like, characterized by many cytoplasmic projections and loss of tight cell-to-cell junctions, whereas control cells under normoxia showed robust cellular junctions with a cobblestone-like, epithelial appearance (Fig. 2A). Acquisition of the mesenchymal-like morphologic phe-

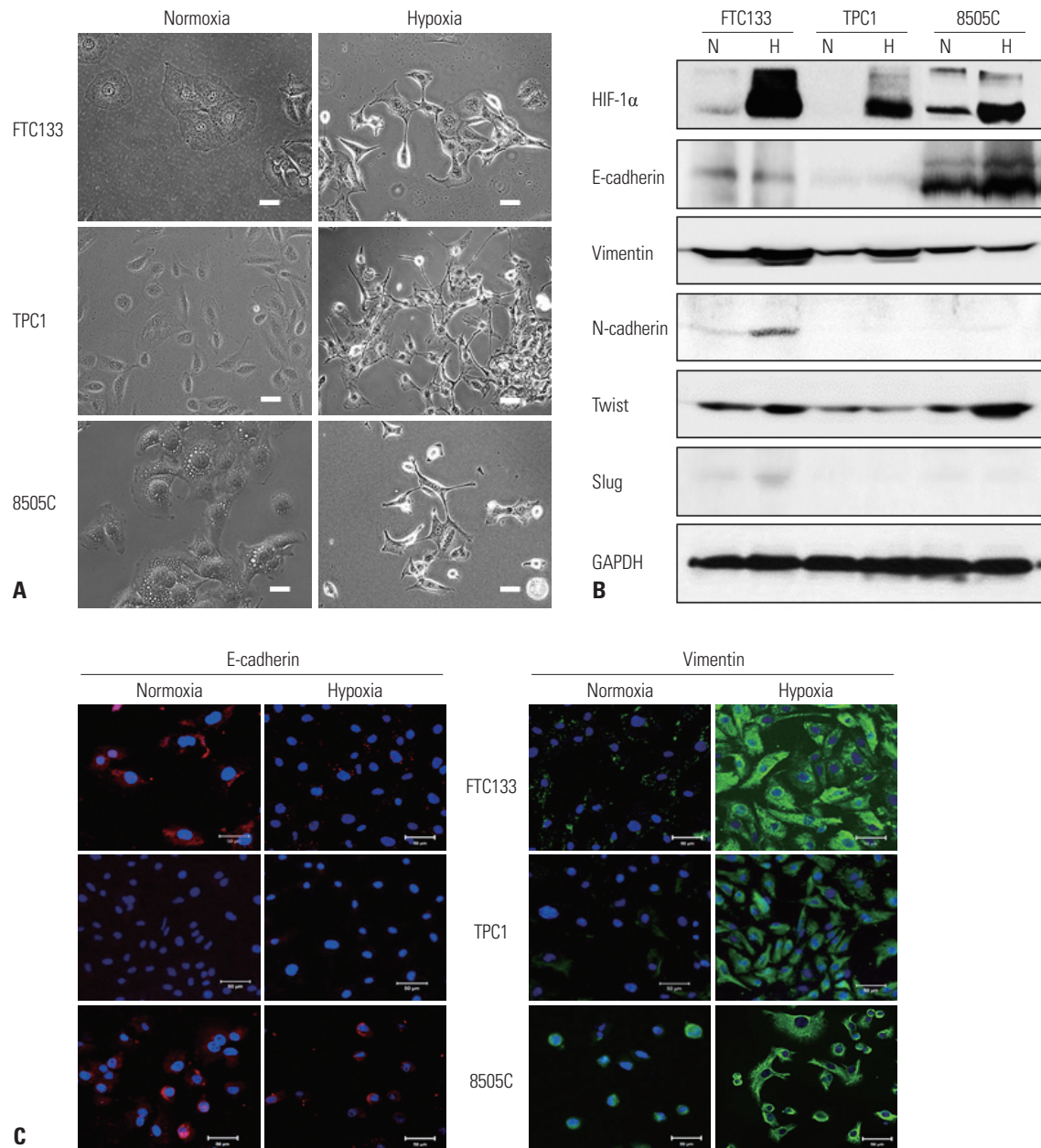


**Fig. 2.** Hypoxia-induced EMT in thyroid cancer cell lines (FTC133, TPC1, and 8505C). All cells were incubated under normoxia or hypoxia (1% O<sub>2</sub>) for 16 h. (A) External cell morphology was analyzed under a phase-contrast microscope. After exposure to hypoxic conditions, cells appeared to be flatter, elongated, and ramified with long extending processes. Loss of cell-to-cell contact was also noted after hypoxia ( $\times 200$ ). Scale bar=50  $\mu$ m. (B) Western blot analysis of signals related to EMT using the indicated antibodies revealed that the expression of a general epithelial marker (E-cadherin) decreased and that of mesenchymal markers (N-cadherin and vimentin) increased under hypoxic conditions. In addition, a downstream transcription factor, Twist, was also increased after hypoxia exposure. (C) Immunofluorescence assays using Alexa 568 (red)- or Alexa 488 (green)-labeled antibodies (1:250) to visualize E-cadherin (red) or vimentin (green), respectively, in each cell line; DAPI was used to label cell nuclei (blue). Changes consistent with the Western blotting results were noted using confocal microscopy and were most intense in FTC133 cells. Scale bar=50  $\mu$ m. Each figure is representative of triplicate experiments. HIF-1 $\alpha$ , hypoxia inducible factor-1 $\alpha$ ; FTC, follicular thyroid cancer; EMT, epithelial-to-mesenchymal transition.

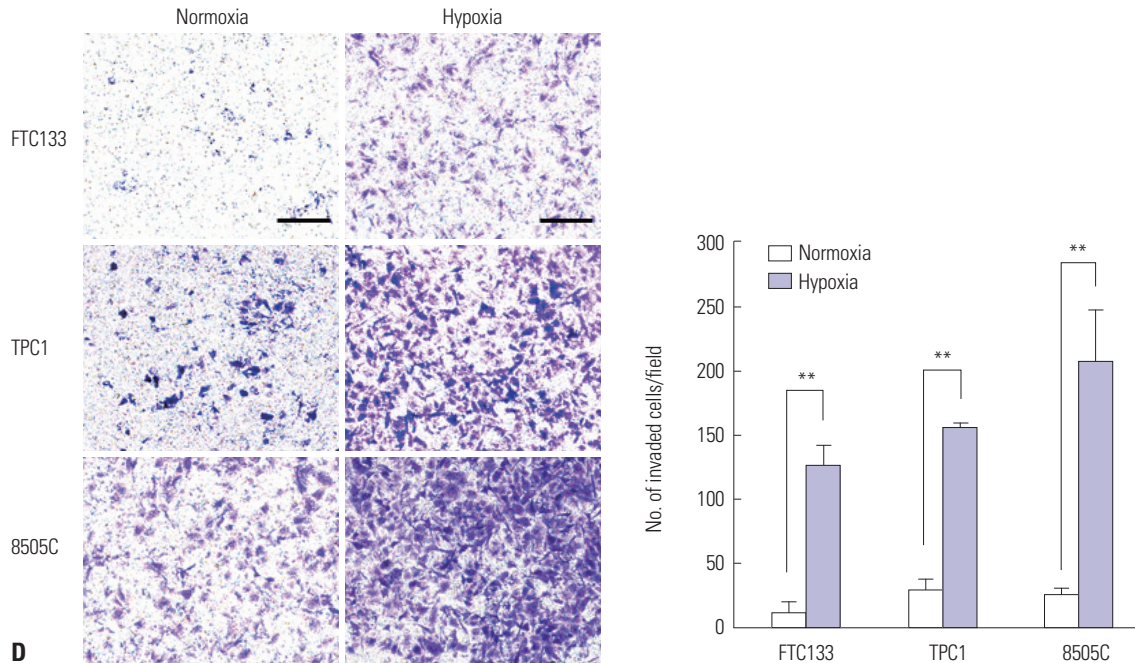


**Fig. 2.** Hypoxia-induced EMT in thyroid cancer cell lines (FTC133, TPC1, and 8505C). All cells were incubated under normoxia or hypoxia (1% O<sub>2</sub>) for 16 h. (D) Transwell invasion assays were performed to evaluate the invasive ability of cells. FTC133, TPC1, and 8505C cells were seeded on a filter (pore size, 8 coated  $\mu$ m) coated with Matrigel in the upper compartment and exposed to a normoxic or hypoxic environment. After 12 h, the cells in the pores or cells attached to the undersurface of the membrane were counted, while those attached to the lower section were stained with crystal violet (panel) and counted using a light microscope (graph) ( $\times$ 200). Scale bar=250  $\mu$ m. The data represent mean $\pm$ SD of three independent experiments. \*\* $p$ <0.01. EMT, epithelial-to-mesenchymal transition; FTC, follicular thyroid cancer.

notype was most apparent in FTC133 cells.

Next, we evaluated EMT-related protein expression (E-cadherin, vimentin, N-cadherin, Twist, and Slug) using Western blot analysis. As shown in Fig. 2B, after 16 h incubation under hypoxia, expression of the epithelial marker E-cadherin was decreased, whereas the expression of mesenchymal markers vimentin and N-cadherin significantly increased in FTC133 cells. Interestingly, the expression of Twist, a master EMT regulator,<sup>24</sup> also markedly increased after exposure to hypoxia in FTC133 cells. Even though another EMT related transcription factor, Slug<sup>25</sup> showed faint expression even under hypoxia, a slight augmentation in expression was noted under hypoxic conditions only in FTC133 cells. Consistent with the immunoblot results, E-cadherin downregulation and vimentin augmentation were noted in the immunofluorescence analysis (Fig. 2C).

**Cells with hypoxia-induced EMT phenotypes show high invasiveness *in vitro***

To investigate whether cells that have undergone hypoxia-induced EMT exhibit changes in invasion ability, a transwell assay was performed to determine single cancer cell invasion. As shown in Fig. 2D, all the thyroid cancer cells were more invasive after exposure to hypoxia. FTC133 cells had more than 12-fold increase in gel invasion ( $p$ <0.01), whereas there was approximately 5-fold and 8-fold increase in TPC1 and 8505C cells, respectively ( $p$ <0.01 and  $p$ <0.01).

**Overexpression of HIF-1 $\alpha$  induces epithelial-to-mesenchymal transition in follicular thyroid cancer**

To determine the association between HIF-1 $\alpha$  expression and EMT in aggressive tumor invasion, we transfected a plasmid (pcDNA3-HIF-1 $\alpha$ ) encoding human HIF-1 $\alpha$  into FTC133 cells, which showed the highest induction of HIF-1 $\alpha$  and acquisition of mesenchymal morphologic characteristics under hypoxia. As shown in Fig. 3A, FTC133 cells transfected with the HIF-1 $\alpha$  vector showed mesenchymal morphologic changes, even under normoxia, similar to those in cells exposed to hypoxic conditions. Interestingly, Western blotting and real-time PCR showed similar changes in EMT marker expression under hypoxia in HIF-1 $\alpha$ -overexpressing FTC133 cells (Fig. 3B and C). In addition, as shown in Fig. 3D, HIF-1 $\alpha$  overexpression alone led to a simultaneous decrease in E-cadherin fluorescence and increase in vimentin fluorescence. Furthermore, as shown by the invasion assay, HIF-1 $\alpha$  overexpression increased the invasiveness of FTC133 cells by approximately 7-fold ( $p$ <0.01) (Fig. 3E).

**Constitutive knockdown of HIF-1 $\alpha$  expression reduced hypoxia-induced epithelial-to-mesenchymal transition in follicular thyroid cancer**

To confirm the significance of HIF-1 $\alpha$  in hypoxia-induced EMT in FTC133 cells, we blocked the HIF-1 $\alpha$  pathway in FTC133 cells by constitutive expression of shRNA. As shown in Fig. 4A and B, HIF-1 $\alpha$  expression was diminished by shRNA under normoxia, and there was little increase in HIF-1 $\alpha$  expression even after

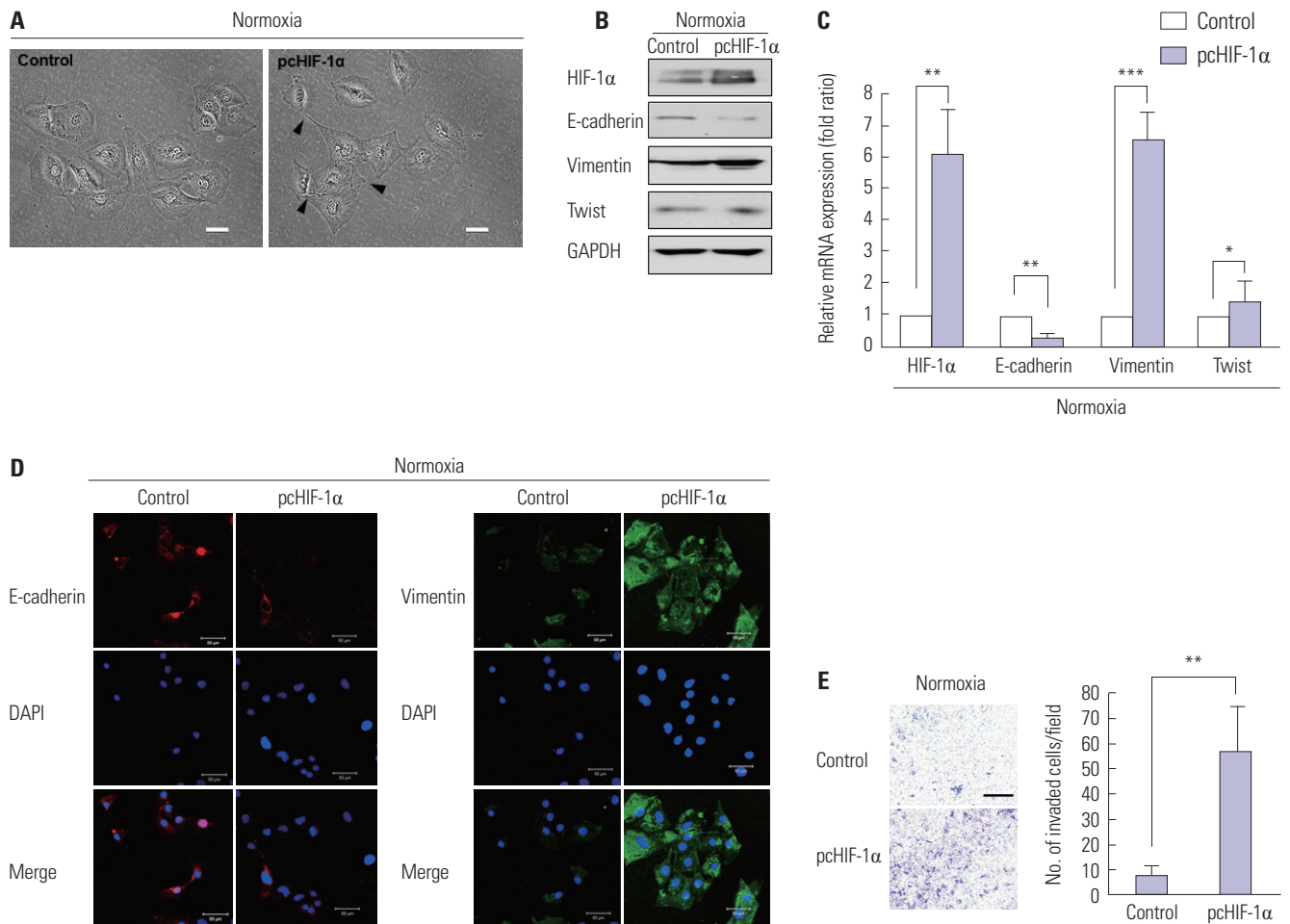


**Fig. 3.** HIF-1 $\alpha$  overexpression promotes EMT in FTC133 cells even under normoxia. FTC133 cells were transfected transiently with either empty vector (Control) or pcDNA3-HIF-1 $\alpha$  (pcHIF-1 $\alpha$ ) and maintained under normoxia. (A) After a 48-hr transfection period, morphological changes in cells were analyzed under a phase-contrast microscope ( $\times 200$ ). HIF-1 $\alpha$  overexpression induced typical EMT morphologic changes, including increased cytoplasmic projection (black arrowheads). Scale bar=50  $\mu$ m. E-cadherin, vimentin, and Twist expression was evaluated by (B) Western blot analysis, (C) real-time PCR using GAPDH as an internal control, and (D) immunofluorescence analysis in HIF-1 $\alpha$ -transfected FTC133 cells. DAPI was used to label cell nuclei (blue). Scale bar=50  $\mu$ m. (E) Transwell invasion assay results revealed that HIF-1 $\alpha$  overexpression significantly increased the invasive ability of FTC133 cells. The panel is representative of triplicate experiments. Scale bar=250  $\mu$ m. Graphs show quantification of the transwell assay. The data represent mean $\pm$ SD of three independent experiments. \* $p$ <0.05, \*\* $p$ <0.01, \*\*\* $p$ <0.001. HIF-1 $\alpha$ , hypoxia inducible factor-1 $\alpha$ ; EMT, epithelial-to-mesenchymal transition; FTC, follicular thyroid cancer.

hypoxic stimulation compared with the LVcontrol. We then assessed whether suppression of HIF-1 $\alpha$  could modulate the expression of EMT markers. As expected, blocking HIF-1 $\alpha$  via shRNA diminished the hypoxia-induced changes in E-cadherin, vimentin, and Twist expression at both the protein and mRNA levels (Fig. 4B and C). Immunofluorescent analysis of E-cadherin and vimentin showed similar results to Western blotting and real-time PCR (Fig. 4D). Moreover, suppression of HIF-1 $\alpha$  expression significantly decreased the number of invasive FTC133 cells compared with the control under hypoxic conditions ( $p=0.003$ ) (Fig. 4E). Fig. 4F demonstrates that under hypoxic conditions, wound closure in LVcontrol FTC133 cells significantly increased (from 1.6- to 4.3-fold), whereas when HIF-1 $\alpha$  was blocked by shRNA, hypoxia-induced wound closure decreased, resulting in no significant changes across the denuded zone between hypoxia and normoxia. These results in-

dicate that HIF-1 $\alpha$  is a crucial molecular signal inducing EMT in FTC133 cells.

### Suppression of HIF-1 $\alpha$ decreased epithelial-to-mesenchymal transition of follicular thyroid cancer in the orthotopic xenograft murine model

To investigate whether the aforementioned results were evident *in vivo*, we used an FTC133 orthotopic xenograft mouse model generated by injection of shHIF-1 $\alpha$  cells or LVcontrol cells into the thyroid gland. All mice survived the experimental period. As Fig. 5A shows, tumors induced by shHIF-1 $\alpha$  cells were significantly smaller in both tumor volume ( $p=0.002$ ) and weight ( $p<0.001$ ) than those induced by LVcontrol cells 28 days after injection. Next, we performed histologic analysis of tumor tissues from each group of animals. Using lower power observations (upper row of Fig. 5B,  $\times 100$ ) after hematoxylin and eo-

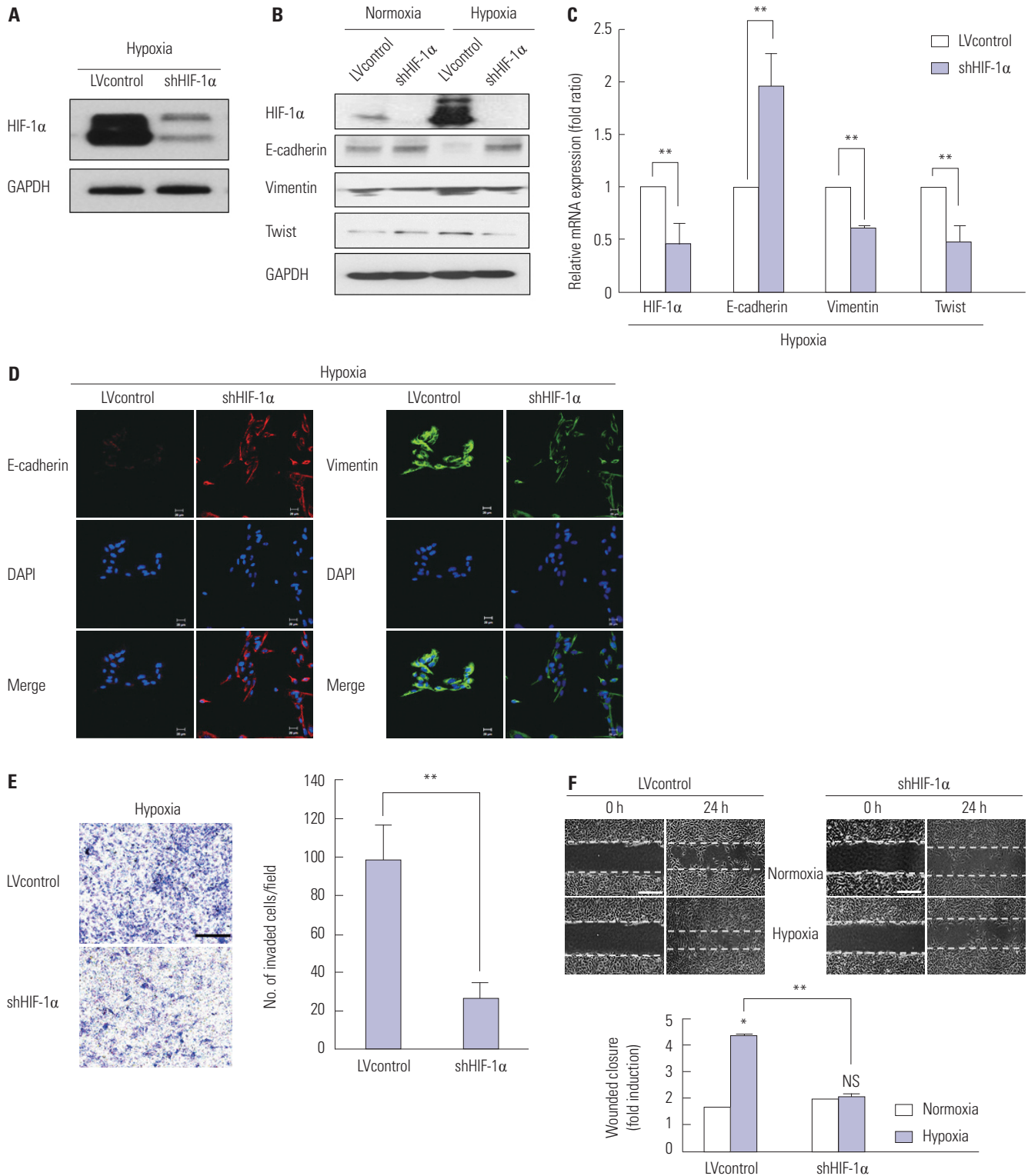


**Fig. 4.** Knockdown of HIF-1 $\alpha$  in FTC133 cells reverses hypoxia-induced EMT. Stable silencing of HIF-1 $\alpha$  was performed using shRNA lentiviral particles (shHIF-1 $\alpha$ ). The lentiviral vector was used as the empty control vector (LVcontrol). All cells were incubated under normoxia or hypoxia (1% O<sub>2</sub>) for 16 h. (A) shHIF-1 $\alpha$  transduction repressed hypoxia-induced HIF-1 $\alpha$  activation in FTC133 cells. HIF-1 $\alpha$  and EMT marker (E-cadherin, vimentin, and Twist) expression was evaluated by (B) Western blot analysis, (C) real-time PCR using GAPDH as an internal control, and (D) immunofluorescence analysis in HIF-1 $\alpha$  knockdown FTC133 cells. DAPI was used to label cell nuclei (blue). Scale bar=20  $\mu$ m. (E) Transwell invasion assay and (F) scratch-wound healing assay revealed that HIF-1 $\alpha$  suppression significantly decreased the invasion and migration of FTC133 cells. Each panel was representative of triplicate experiments. Scale bars=250  $\mu$ m and 200  $\mu$ m, respectively. Graphs show quantification of each assay. The data represent mean $\pm$ SD of three independent experiments. \* $p$ <0.05, \*\* $p$ <0.01. HIF-1 $\alpha$ , hypoxia inducible factor-1 $\alpha$ ; EMT, epithelial-to-mesenchymal transition; FTC, follicular thyroid cancer; LVcontrol, lentiviral control; NS, not significant.

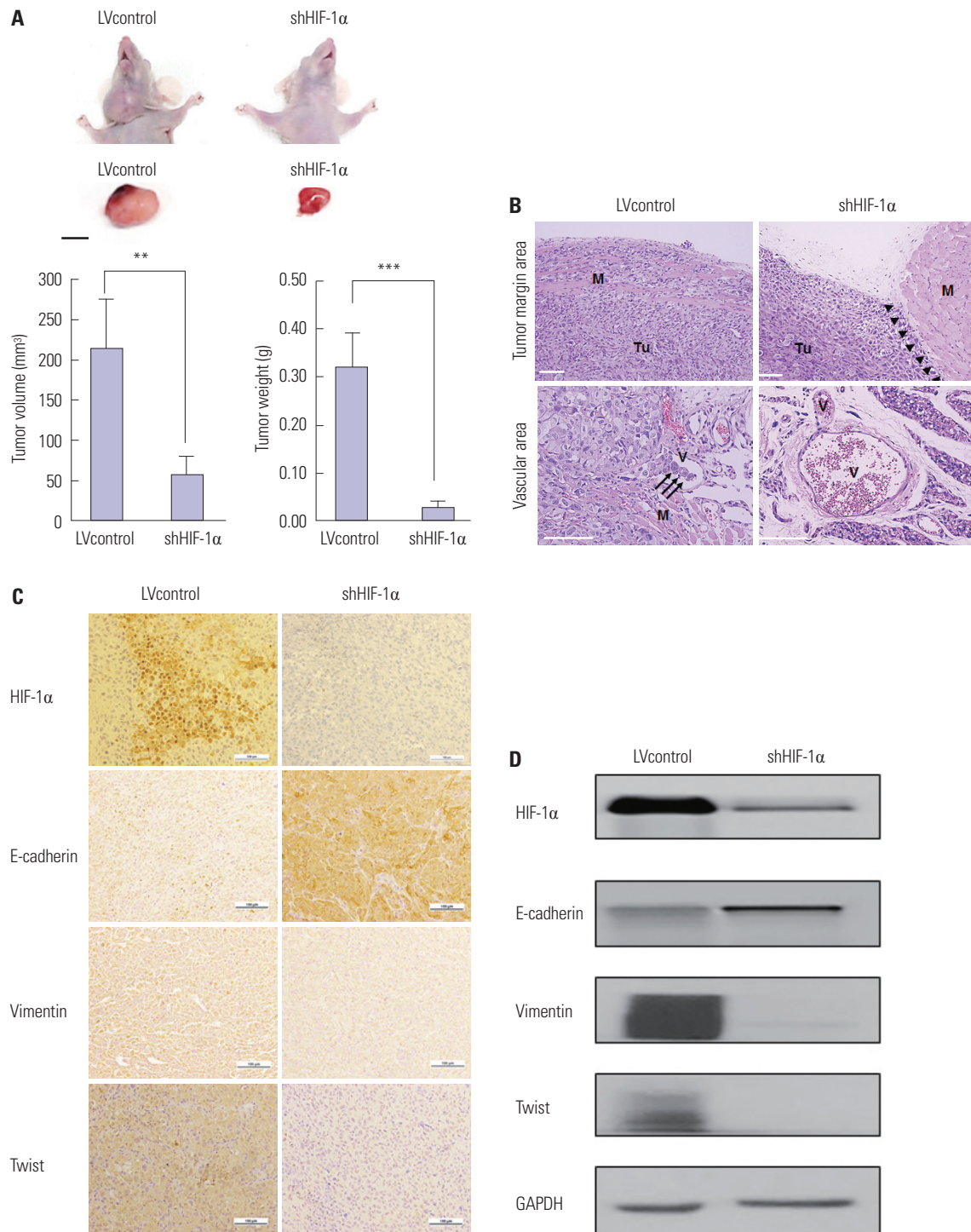


**Fig. 5.** Knockdown of HIF-1α by specific shRNA reduces EMT in an orthotopic FTC murine model. To determine whether the aforementioned results were evident *in vivo*, stable shHIF-1α FTC133 cells ( $1 \times 10^5$ /mouse) were injected into the right side of the thyroid gland in 6-week-old male nude mice (n=5). Twenty-eight days after inoculation with FTC133 cells, tumors were harvested for Western blotting and histologic evaluations including H&E staining and immunohistochemical analysis. (A) Representative image of tumors. Tumors derived from shHIF-1α cells showed significantly decreased tumor volume and weight compared with that from LVcontrol cells. Scale bar=10 mm. (B) H&E stain of tumor derived LVcontrol cells showed more invasive features than that from shHIF-1α cells. Upper panel ( $\times 100$ ): tumors derived from shHIF-1α cells had a clear boundary between the tumor and adjacent nontumor tissue (arrowheads), whereas tumors induced by LVcontrol cells demonstrated irregular invasive fronts. Lower panel ( $\times 200$ ): tumor cell invasions into blood vessel forming tumor embolis (arrows) are noted in the tissue from LVcontrol group, whereas no definite tumor emboli in that from shHIF-1α group. Scale bar=50 μm. (C) Representative immunohistochemical results showed more intense staining of E-cadherin, but weaker staining of vimentin and Twist, supporting the *in vitro* results. Scale bar=100 μm. (D) Western blot analysis of HIF-1α, E-cadherin, vimentin, and Twist showed similar changes to those seen *in vitro*. \*\* $p < 0.01$ , \*\*\* $p < 0.001$ . M, muscle; Tu, tumor; V, vessel; HIF-1α, hypoxia inducible factor-1α; EMT, epithelial-to-mesenchymal transition; FTC, follicular thyroid cancer; LVcontrol, lentiviral control; H&E, hematoxylin and eosin.

sin staining, tumor from LV control group showed more aggressive feature of infiltration to adjacent muscles whereas that from shHIF-1 $\alpha$  group maintained clear demarcation from surrounding muscle (arrowhead). In addition, we found frequent vascular invasion of tumor embolis (arrow, lower row of Fig. 5B,  $\times 200$ ) in the vascular area of specimens from LVcontrol group, whereas no vascular invasion was identified tumors from shHIF-1 $\alpha$  group. Tumor tissue sections were then stained to determine the expression of HIF-1 $\alpha$ , E-cadherin, vimentin, and Twist. Tumor tissues derived from shHIF-1 $\alpha$  FTC133 cells showed markedly stronger E-cadherin staining and weaker vimentin and Twist staining compared with that from LVcontrol group (Fig. 5C). Furthermore, as shown in Fig. 5D, tumor tissues derived from shHIF-1 $\alpha$  cells had markedly lower expressions of HIF-1 $\alpha$ , vimentin, and Twist, and increased expression of E-cadherin compared with the LVcontrol. These data are consistent with the *in vitro* findings, suggesting that HIF-1 $\alpha$  induces EMT, which is associated with Twist in FTC cells, even without hypoxia.

## DISCUSSION

Cancer cell invasion or metastasis to other tissues or organs leads to a decrease in prognosis and survival.<sup>26</sup> For this, identifying and controlling the mechanisms of invasion or metastasis remains one of the main foci of cancer therapeutics. Although increasing evidence suggests that activation of the Ras-Raf-Mek-ERK pathway is important in the development of PTC,<sup>21,27</sup> the molecular mechanism contributing to FTC is poorly defined.<sup>16</sup> A number of genetic abnormalities have been reported in human FTCs, such as mutations in *RAS*,<sup>28</sup> *PAX8-PPAR $\gamma$*  rearrangement,<sup>29</sup> and *PTEN*,<sup>30</sup> and *Prkar1a* deletion.<sup>31</sup> However, the association of these mutations with tumorigenesis and aggressive features is less clear, because tumor development is unreliable and does not exhibit distant metastasis, which is a typical feature of human FTC.<sup>30</sup> In this study, we showed that HIF-1 $\alpha$  plays a crucial role in the migration and invasion of FTC via triggering EMT *in vivo* orthotopic FTC murine model, as well as *in vitro*.

HIF-1, which is a heterodimer complex containing two basic helix-loop-helix (bHLH) transcription factors (HIF-1 $\alpha$  and HIF-1 $\beta$ ), is the main responder to hypoxia.<sup>16,18</sup> Under hypoxic conditions, stabilized HIF-1 $\alpha$  translocates from the cytoplasm to the nucleus to dimerize with HIF-1 $\beta$  and activates downstream target genes that contribute to cancer progression and promote tumor aggressiveness, leading to metastasis or resistance to therapy.<sup>19</sup> Intratumoral hypoxia followed by HIF-1 $\alpha$  overexpression is associated with tumor invasiveness and metastasis in various cancers.<sup>15,20</sup> In our study, among the cell lines examined, HIF-1 $\alpha$  was significantly activated under hypoxia in FTC133 cell line, even though basal expression levels were higher in ATC cells. This observation is in accordance with previous work by Jubb, et al.<sup>32</sup> who reported particularly high expression levels of HIF-1 $\alpha$  in FTCs.<sup>16</sup> The highly induced activa-

tion of HIF-1 $\alpha$  by hypoxia may be supported by *PTEN* loss in FTC133 cell line.<sup>30</sup> Increasing evidence suggests that *PTEN* loss is involved in HIF-1 $\alpha$  regulation and in aggressiveness, therapeutic resistance, and metastasis of cancer.<sup>33,34</sup> Moreover, Burrows, et al.<sup>10</sup> showed that reintroduction of *PTEN* into cells reduced HIF-1 $\alpha$  activity.

The transition of an epithelial carcinoma to a mesenchymal phenotype (EMT) is characterized by immense morphologic changes marked by loss of polarity and cell-to-cell contacts, and an enhanced ability to migrate through the neighboring extracellular matrix.<sup>8</sup> The molecular hallmarks for EMT are downregulation of epithelial cell cadherin molecules, such as E-cadherin, and upregulation of mesenchymal components, such as vimentin and N-cadherin.<sup>35</sup> In the present study, thyroid cancer cells, especially FTC133 cells, showed typical EMT morphologic changes under hypoxic stress, implying that hypoxia induces EMT. This was confirmed by changes in molecular marker expression, including a cadherin switch (decrease of E-cadherin, increase of N-cadherin). Cadherin switch, a hallmark of EMT, was reported to play an important role in promoting cell mobility and invasion.<sup>9</sup> Many solid tumor cells have been observed to undergo a cadherin switch, which was suggested to be part of the initial tumor invasion cascade.<sup>36,37</sup> Moreover, these changes augmented the ability of cells to invade and migrate, which is regulated by HIF-1 $\alpha$  overexpression or suppression. These data suggest that HIF-1 $\alpha$  could regulate EMT in FTC133 cells independent of oxygen condition.

Multifarious transcriptional factors, including Snail,<sup>38</sup> Slug,<sup>39</sup> Twist,<sup>24</sup> Zeb1,<sup>40</sup> SIP1,<sup>41</sup> and E47,<sup>42</sup> were shown to induce EMT through the cadherin switch and are perceived as EMT regulators.<sup>38</sup> In this study, we showed that Twist expression was increased by hypoxic stress. Interestingly, overexpression of HIF-1 $\alpha$  alone augmented the expression of Twist, while suppression of HIF-1 $\alpha$  abolished the hypoxia-induced increases in Twist expression in FTC133 cells, suggesting that Twist is regulated by HIF-1 $\alpha$  in this cell line. Twist is another bHLH transcription factor and one of the master regulators of the EMT process.<sup>43</sup> The gene for Twist (*TWIST1*) is located on human chromosome 7p21.<sup>44</sup> Since Yang, et al.<sup>24</sup> initially reported Twist as be an essential factor in cancer metastasis, more evidence has demonstrated associations of Twist with a more aggressive phenotype and a worse prognosis in human cancers via Twist-induced EMT.<sup>43,45</sup> As expected by its EMT-inducing capabilities, Twist causes the tumor cells to switch to extravasation, associated with the formation of membrane protrusions, resulting in intravascular migration and extravasation through the vessel wall, which is essential to the metastatic process.<sup>46</sup> Moreover, Twist is capable of promoting the formation of invadopodia, specialized membrane protrusions for extracellular matrix degradation.<sup>47</sup> The morphologic changes observed in the present study are consistent with the Twist-associated tumor cell changes typically seen during the EMT process.

Recent studies demonstrated that HIF-1 $\alpha$  and Twist are part

of the same pathway that regulates cancer invasion and metastasis.<sup>24</sup> Moreover, Twist is a direct target of HIF-1 $\alpha$  with a functional HRE present in the promoter of the Twist gene.<sup>45</sup> In addition, several studies showed that co-expression of HIF-1 $\alpha$  and Twist is involved in metastasis and poor prognosis in several cancers.<sup>43,48</sup> To the best of our knowledge, we are the first to report that HIF-1 $\alpha$  mediates hypoxic responses and promotes EMT through upregulation of Twist expression in FTC cells. These observations were confirmed *in vivo* using an orthotopic xenograft FTC model.

In conclusion, this study demonstrates that HIF-1 $\alpha$  plays a crucial role in hypoxia-induced EMT in FTC133 cells. Moreover, the molecular mechanism involves Twist signaling and its regulation by HIF-1 $\alpha$ . These results suggest that HIF-1 $\alpha$  and Twist are promising molecular targets that may contribute to novel strategies against aggressive and metastatic FTC.

## ACKNOWLEDGEMENTS

This study was supported by a faculty research grant of Yonsei University College of Medicine for 2010 (6-2010-0028) and a grant from the National Research Foundation of Korea (NRF) grant (2012R1A1A2042666).

## REFERENCES

- Phay JE, Ringel MD. Metastatic mechanisms in follicular cell-derived thyroid cancer. *Endocr Relat Cancer* 2013;20:R307-19.
- Carling T, Udelsman R. Thyroid cancer. *Annu Rev Med* 2014;65:125-37.
- Chang JW, Kang SU, Shin YS, Kim KI, Seo SJ, Yang SS, et al. Non-thermal atmospheric pressure plasma inhibits thyroid papillary cancer cell invasion via cytoskeletal modulation, altered MMP-2/-9/uPA activity. *PLoS One* 2014;9:e92198.
- Rahmani N, Abbas Hashemi S, Fazli M, Raisian M. Clinical management and outcomes of papillary, follicular and medullary thyroid cancer surgery. *Med Glas (Zenica)* 2013;10:164-7.
- Zhao JH, Luo Y, Jiang YG, He DL, Wu CT. Knockdown of  $\beta$ -Catenin through shRNA cause a reversal of EMT and metastatic phenotypes induced by HIF-1 $\alpha$ . *Cancer Invest* 2011;29:377-82.
- Xiao W, Jiang M, Li H, Li C, Su R, Huang K. Knockdown of FAK inhibits the invasion and metastasis of Tca8113 cells in vitro. *Mol Med Rep* 2013;8:703-7.
- Marie-Egyptienne DT, Lohse I, Hill RP. Cancer stem cells, the epithelial to mesenchymal transition (EMT) and radioresistance: potential role of hypoxia. *Cancer Lett* 2013;341:63-72.
- De Craene B, Bex G. Regulatory networks defining EMT during cancer initiation and progression. *Nat Rev Cancer* 2013;13:97-110.
- Cavallaro U, Christofori G. Cell adhesion and signalling by cadherins and Ig-CAMs in cancer. *Nat Rev Cancer* 2004;4:118-32.
- Burrows N, Resch J, Cowen RL, von Wasielewski R, Hoang-Vu C, West CM, et al. Expression of hypoxia-inducible factor 1 alpha in thyroid carcinomas. *Endocr Relat Cancer* 2010;17:61-72.
- Kim DH, Hossain MA, Kim MY, Kim JA, Yoon JH, Suh HS, et al. A novel resveratrol analogue, HS-1793, inhibits hypoxia-induced HIF-1 $\alpha$  and VEGF expression, and migration in human prostate cancer cells. *Int J Oncol* 2013;43:1915-24.
- Melstrom LG, Salabat MR, Ding XZ, Strouch MJ, Grippo PJ, Mirzoeva S, et al. Apigenin down-regulates the hypoxia response genes: HIF-1 $\alpha$ , GLUT-1, and VEGF in human pancreatic cancer cells. *J Surg Res* 2011;167:173-81.
- Kockar F, Yildirim H, Sagkan RI, Hagemann C, Soysal Y, Anacker J, et al. Hypoxia and cytokines regulate carbonic anhydrase 9 expression in hepatocellular carcinoma cells in vitro. *World J Clin Oncol* 2012;3:82-91.
- Sendoel A, Kohler I, Fellmann C, Lowe SW, Hengartner MO. HIF-1 antagonizes p53-mediated apoptosis through a secreted neuronal tyrosinase. *Nature* 2010;465:577-83.
- Culver C, Melvin A, Mudie S, Rocha S. HIF-1 $\alpha$  depletion results in SP1-mediated cell cycle disruption and alters the cellular response to chemotherapeutic drugs. *Cell Cycle* 2011;10:1249-60.
- Burrows N, Babur M, Resch J, Williams KJ, Brabant G. Hypoxia-inducible factor in thyroid carcinoma. *J Thyroid Res* 2011;2011:762905.
- Li H, Liang CZ, Chen QX. Regulatory role of hypoxia inducible factor in the biological behavior of nucleus pulposus cells. *Yonsei Med J* 2013;54:807-12.
- Semenza GL. HIF-1: upstream and downstream of cancer metabolism. *Curr Opin Genet Dev* 2010;20:51-6.
- Semenza GL. Targeting HIF-1 for cancer therapy. *Nat Rev Cancer* 2003;3:721-32.
- Warfel NA, El-Deiry WS. HIF-1 signaling in drug resistance to chemotherapy. *Curr Med Chem* 2014;21:3021-8.
- Zerilli M, Zito G, Martorana A, Pitrone M, Cabibi D, Cappello F, et al. BRAF(V600E) mutation influences hypoxia-inducible factor-1alpha expression levels in papillary thyroid cancer. *Mod Pathol* 2010;23:1052-60.
- Kim CH, Kwon S, Bahn JH, Lee K, Jun SI, Rack PD, et al. Effects of atmospheric nonthermal plasma on invasion of colorectal cancer cells. *Appl Phys Lett* 2010;96:243701.
- Chang JW, Kang SU, Choi JW, Shin YS, Baek SJ, Lee SH, et al. Tolfenamic acid induces apoptosis and growth inhibition in anaplastic thyroid cancer: involvement of nonsteroidal anti-inflammatory drug-activated gene-1 expression and intracellular reactive oxygen species generation. *Free Radic Biol Med* 2014;67:115-30.
- Yang J, Mani SA, Donaher JL, Ramaswamy S, Itzykson RA, Come C, et al. Twist, a master regulator of morphogenesis, plays an essential role in tumor metastasis. *Cell* 2004;117:927-39.
- Carpenter RL, Paw I, Dewhirst MW, Lo HW. Akt phosphorylates and activates HSF-1 independent of heat shock, leading to Slug overexpression and epithelial-mesenchymal transition (EMT) of HER2-overexpressing breast cancer cells. *Oncogene* 2015;34:546-57.
- Chen L, Shi Y, Yuan J, Han Y, Qin R, Wu Q, et al. HIF-1 alpha overexpression correlates with poor overall survival and disease-free survival in gastric cancer patients post-gastrectomy. *PLoS One* 2014;9:e90678.
- Friday BB, Adjei AA. Advances in targeting the Ras/Raf/MEK/Erk mitogen-activated protein kinase cascade with MEK inhibitors for cancer therapy. *Clin Cancer Res* 2008;14:342-6.
- Vasko V, Ferrand M, Di Cristofaro J, Carayon P, Henry JF, de Micco C. Specific pattern of RAS oncogene mutations in follicular thyroid tumors. *J Clin Endocrinol Metab* 2003;88:2745-52.
- Nikiforova MN, Lynch RA, Biddinger PW, Alexander EK, Dorn GW 2nd, Tallini G, et al. RAS point mutations and PAX8-PPAR gamma rearrangement in thyroid tumors: evidence for distinct molecular pathways in thyroid follicular carcinoma. *J Clin Endocrinol Metab* 2003;88:2318-26.
- Burrows N, Babur M, Resch J, Ridsdale S, Mejin M, Rowling EJ, et al. GDC-0941 inhibits metastatic characteristics of thyroid carcinomas by targeting both the phosphoinositide-3 kinase (PI3K) and hypoxia-inducible factor-1 $\alpha$  (HIF-1 $\alpha$ ) pathways. *J Clin Endocrinol Metab*

- 2011;96:E1934-43.
31. Sandrini F, Matyakhina L, Sarlis NJ, Kirschner LS, Farmakidis C, Gimm O, et al. Regulatory subunit type I-alpha of protein kinase A (PRKAR1A): a tumor-suppressor gene for sporadic thyroid cancer. *Genes Chromosomes Cancer* 2002;35:182-92.
  32. Jubb AM, Pham TQ, Hanby AM, Frantz GD, Peale FV, Wu TD, et al. Expression of vascular endothelial growth factor, hypoxia inducible factor 1alpha, and carbonic anhydrase IX in human tumours. *J Clin Pathol* 2004;57:504-12.
  33. Zundel W, Schindler C, Haas-Kogan D, Koong A, Kaper F, Chen E, et al. Loss of PTEN facilitates HIF-1-mediated gene expression. *Genes Dev* 2000;14:391-6.
  34. Maxwell PJ, Coulter J, Walker SM, McKechnie M, Neisen J, McCabe N, et al. Potentiation of inflammatory CXCL8 signalling sustains cell survival in PTEN-deficient prostate carcinoma. *Eur Urol* 2013;64:177-88.
  35. Franco-Chuaire ML, Magda Carolina SC, Chuaire-Noack L. Epithelial-mesenchymal transition (EMT): principles and clinical impact in cancer therapy. *Invest Clin* 2013;54:186-205.
  36. Gravdal K, Halvorsen OJ, Haukaas SA, Akslen LA. A switch from E-cadherin to N-cadherin expression indicates epithelial to mesenchymal transition and is of strong and independent importance for the progress of prostate cancer. *Clin Cancer Res* 2007;13:7003-11.
  37. Fan M, Liu Y, Xia F, Wang Z, Huang Y, Li J, et al. Increased expression of EphA2 and E-N cadherin switch in primary hepatocellular carcinoma. *Tumori* 2013;99:689-96.
  38. Cano A, Pérez-Moreno MA, Rodrigo I, Locascio A, Blanco MJ, del Barrio MG, et al. The transcription factor snail controls epithelial-mesenchymal transitions by repressing E-cadherin expression. *Nat Cell Biol* 2000;2:76-83.
  39. Hajra KM, Chen DY, Fearon ER. The SLUG zinc-finger protein represses E-cadherin in breast cancer. *Cancer Res* 2002;62:1613-8.
  40. Grooteclaes ML, Frisch SM. Evidence for a function of CtBP in epithelial gene regulation and anoikis. *Oncogene* 2000;19:3823-8.
  41. Comijn J, Berx G, Vermassen P, Verschuere K, van Grunsven L, Bruyneel E, et al. The two-handed E box binding zinc finger protein SIP1 downregulates E-cadherin and induces invasion. *Mol Cell* 2001;7:1267-78.
  42. Perez-Moreno MA, Locascio A, Rodrigo I, Dhondt G, Portillo F, Nieto MA, et al. A new role for E12/E47 in the repression of E-cadherin expression and epithelial-mesenchymal transitions. *J Biol Chem* 2001;276:27424-31.
  43. Yang MH, Wu KJ. TWIST activation by hypoxia inducible factor-1 (HIF-1): implications in metastasis and development. *Cell Cycle* 2008;7:2090-6.
  44. Khan MA, Chen HC, Zhang D, Fu J. Twist: a molecular target in cancer therapeutics. *Tumour Biol* 2013;34:2497-506.
  45. Yang MH, Wu MZ, Chiou SH, Chen PM, Chang SY, Liu CJ, et al. Direct regulation of TWIST by HIF-1alpha promotes metastasis. *Nat Cell Biol* 2008;10:295-305.
  46. Stoletoev K, Kato H, Zardoujian E, Kelber J, Yang J, Shattil S, et al. Visualizing extravasation dynamics of metastatic tumor cells. *J Cell Sci* 2010;123(Pt 13):2332-41.
  47. Eckert MA, Yang J. Targeting invadopodia to block breast cancer metastasis. *Oncotarget* 2011;2:562-8.
  48. Hung JJ, Yang MH, Hsu HS, Hsu WH, Liu JS, Wu KJ. Prognostic significance of hypoxia-inducible factor-1alpha, TWIST1 and Snail expression in resectable non-small cell lung cancer. *Thorax* 2009;64:1082-9.